4 CURE CHARACTERISATION: CUREMETER

The first of the methods used to characterise the cure of all the systems was the Strathclyde Curemeter. Cure is associated with an increase in the molar mass of the species present, and changes in the rheology of the liquid resin reflect these changes. This method allowed continuous measurement of the rheology of the reactive mixture during the cure process. The measurements were performed isothermally, and the temperature of the sample was monitored to ensure that the reaction mixture did not exotherm during the course of the cure process. Analysis of the data allowed the gel and vitrification times to be determined. The gel time has been previously defined as the time taken to reach a viscosity of 10^4 Pa s, and the vitrification time as the time taken for the real and imaginary amplitude plots to return to a baseline. The times to gelation and vitrification were then used to calculate the activation energy for each process.

4.1 STRATHCLYDE MODEL SYSTEM

Since many of the systems studied were complex blends of components, a simple resin system was studied as a model to assist interpretation of subsequent data. This system was a bisphenol-A/F-based (DGEBA/F) epoxy with triethylenetetramine (TETA) as the curing agent. TETA is an aliphatic amine with primary amines at either end of the chain as well as two secondary amines along the backbone of the chain, giving six hydrogen sites that can take part in the reaction - two primary and four secondary (the second hydrogen on each of the terminal positions becomes secondary when the neighbouring hydrogen is deemed as being primary). In general, the reactivity of the primary amine is significantly higher than the secondary amine and hence the initial reaction would be expected to be a simple linear chain extension process, increasing the molar mass and the viscosity of the resin. As cure proceeds, reaction of the secondary amines will initially create a branched chain structure, and it is only in the latter stages of the cure that a three-dimensional cross-linked matrix

(gel) will be formed. The aliphatic amines within this study were chosen as they cure readily at room temperature – allowing study at a range of temperatures.

Prepared samples were cured within a sample vial, and monitored using the Strathclyde curemeter, at room temperature (the oil bath was set at 23°C for this to maintain a constant temperature), 25°C, 30°C, 35°C, 40°C, 45°C and 50°C. The plots of both the real and imaginary amplitudes from the curemeter measurements are given in Figure 1. As the cure temperature increased the time for the both the drop in the amplitude of the real component, and for the imaginary amplitude traces to reach a maximum before returning to baseline, decreased as expected. The amplitude data set was converted to viscosity plots (Figure 2) using a macro built in to the Origin software, which is based on the equations given in *Chapter2, Section 2.1.4*.

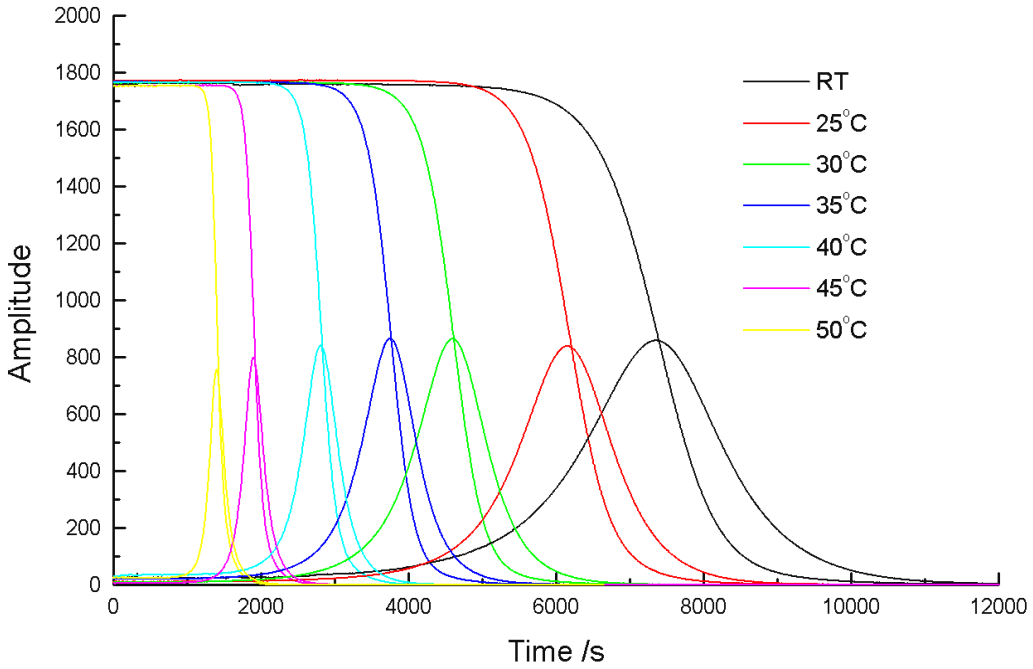

Figure 1. Amplitude plot against cure time, from curemeter data, for the Strathclyde model system at a range of cure temperatures.

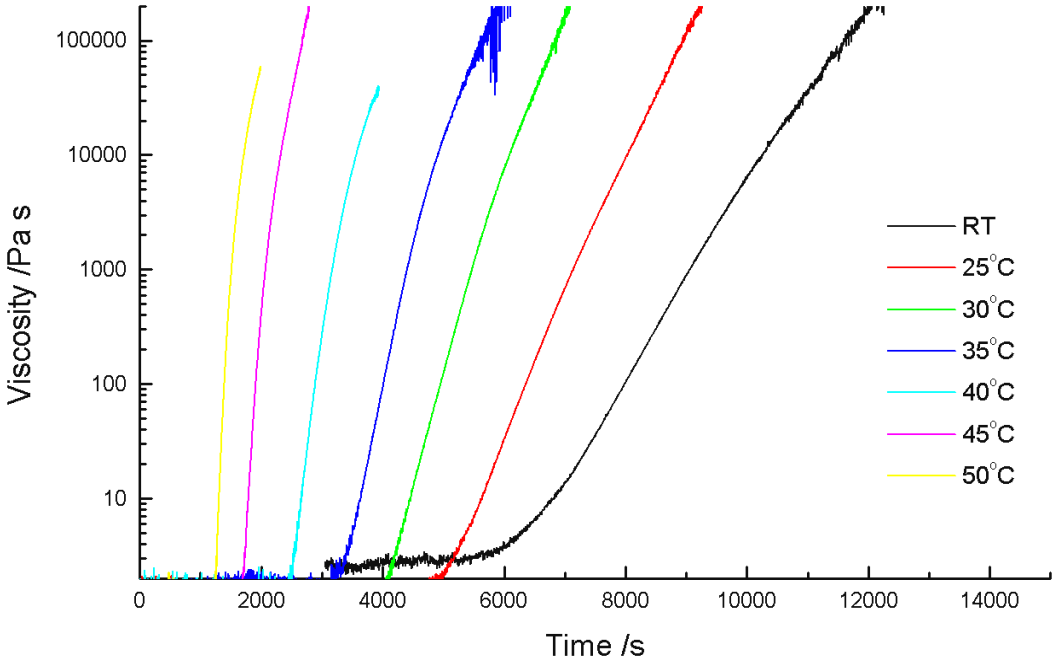

Figure 2. Viscosity profile plot against cure time, from curemeter data, for the Strathclyde model system at a range of cure temperatures.

Figure 2 indicates that for a significant period of the cure process the viscosity of the system does not change. In a condensation type of polymerisation process, such as for epoxy resins, about half of the entities require to have reacted in order for the molar mass to have doubled. For the viscosity to be enhanced a fairly high degree of reaction has to have been achieved and this is reflected in the long time period before there is a significant rise in the viscosity. The apparent simplicity of the shape of the curve implies that the viscosity, and hence molar mass, rises smoothly to a point where gelation occurs. Studies of the cure in other systems have shown that the viscosity-time curves can take on different shapes which may reflect the formation of an entangled matrix prior to total gelation of the material.

The times to gelation and vitrification, for each temperature, are plotted in Figure 3 against the cure temperature. The time to gelation was calculated as the time when the viscosity reached 10^4 Pa s. The arbitrary value of 10^4 Pa s for when gelation occurs is used throughout this chapter and was based on research done using the Strathclyde curemeter [1-3]. Other researchers may choose to use the time at the

imaginary peak maximum, or the point where the real and imaginary lines intersect, and so the gelation activation energies calculated in this chapter are only true for when gelation is taken to occur at 10^4 Pa s. The time to vitrification is taken as the time when both the real and imaginary amplitude plots have returned to a steady baseline, and so the vitrification activation energies calculated are only true under these conditions. The time to the peak maximum is also plotted to illustrate the difference between this method of defining gelation and that of when the viscosity reaches 10^4 Pa s. Figure 3, as well as showing decreasing cure time with increasing cure temperature, also shows that the difference in the time to gelation (at 10^4 Pa s or at the peak maximum) and vitrification decreases with increasing cure temperature.

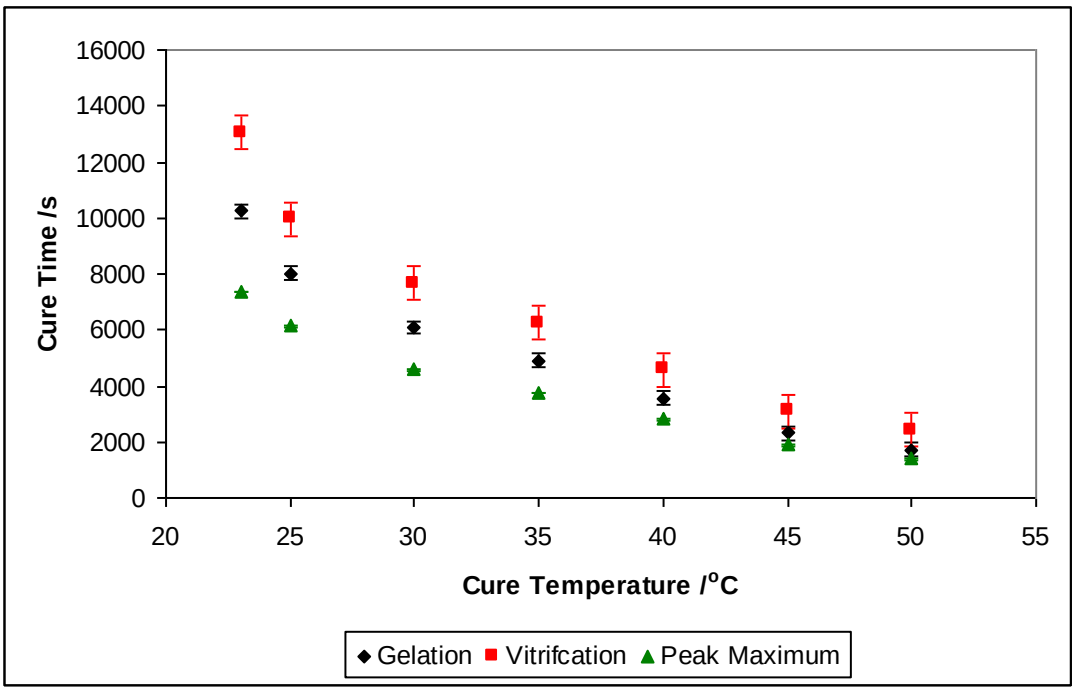

Figure 3. Plot showing effect of cure temperature on cure time for Strathclyde model system.

The natural logs of (the reciprocal of) the gel time and the vitrification time were plotted against the temperature, in Kelvin, as shown in Figure 4. An activation energy, E_a, was found by multiplying the slope of the plot by the gas constant, R (8.314 J K^{-1} mol^{-1}).

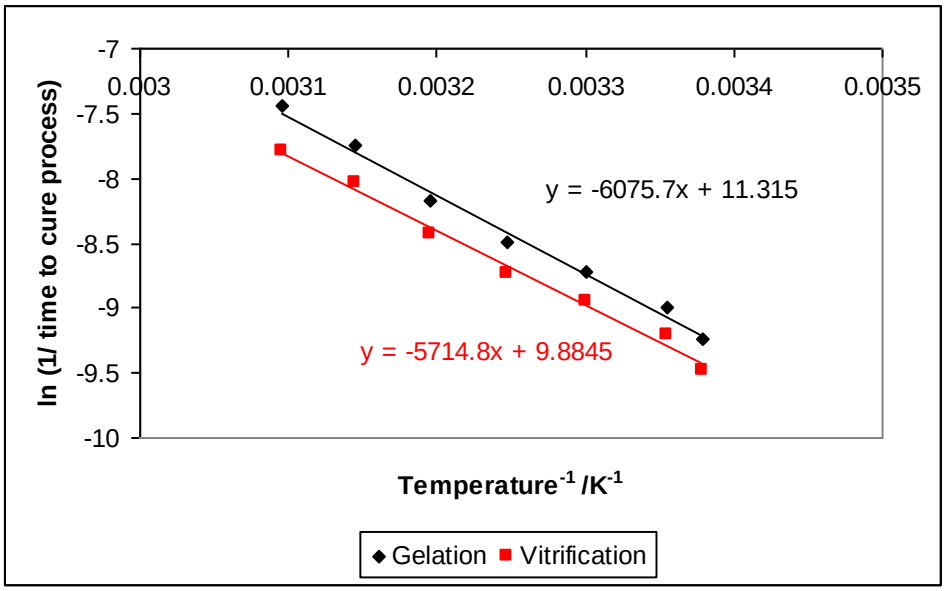

Figure 4. Arrhenius plot for the Strathclyde model system based on gelation and vitrification times calculated from Strathclyde curemeter data.

The main errors associated with the curemeter results are: the temperature of the oil bath (± 2°C), temperature fluctuations due to the effects of the sample exotherm, any slight differences in the area of the paddle, inhomogenous sampling, the time taken from mixing of epoxy/amine to the first reading (less than ten minutes) and the determination of the gelation and vitrification points. The gel time value taken when the viscosity is 10^4 Pa s has an error of *ca.* ±240 s. It was particularly difficult to define the vitrification time as the baseline signal is fairly noisy, and the associated error can be taken as *ca.* ±600 s. Using these values, activation energies were calculated for the time to gelation/vitrification, the time plus the error and time minus the error, and these gave an error for the gelation and vitrification activation energies as ±1.4 kJ mol^{-1} and ±2.8 kJ mol^{-1} respectively. Taking into account the other sources of error described above, the error in the calculation of the gelation activation energy was taken to be ±2.0 kJ mol^{-1}, and ±5.0 kJ mol^{-1} for the vitrification results. These errors will be used throughout this chapter.

Therefore the activation energies calculated from the curemeter measurements were found to be:

$$\mathbf{E_a\ (gelation) = 50.5 \pm 2.0\ kJ\ mol^{-1}}$$

$$\mathbf{E_a\ (vitrification) = 47.5 \pm 5.0\ kJ\ mol^{-1}}$$

The activation energy for gelation when the cure time at the peak maximum is used is 47.3 ± 0.5 kJ mol^{-1}, where the error involved was *ca.* ±30 s which appears to be much lower than the errors associated with the gelation and vitrification times. However it was felt from previous work carried out in the research group that the most appropriate definition of gelation for the particular instrument used was at a set value of viscosity.

It is interesting that despite the complexity of the reaction process a very linear activation plot is observed for this system. The initial reaction would be expected to be dominated by the reaction of the primary amine with the epoxy whereas the subsequent reactions will be controlled by the slower reaction of the secondary amine with the epoxy. It should however be noted that the viscosity will only increase once the molar mass of the species present has risen above a value of ~10^3 g $mol^{-1}$and gelation implies the molar mass approaching infinity. It is probable that the temperature dependence will be influenced to a large extent by the reactivity of the secondary amine which is present in a ratio of 2:1 in this curing system. It may also be noted that it would not be expected that the complicating side reaction of a hydroxyl initiated cure would make a significant contribution to the polymerisation process. The latter is known to contribute to the cure process towards the end of the reaction when the concentration of hydroxyl groups has become large and is also catalysed by the presence of tertiary amines, where tertiary amines are produced when the secondary amines have reacted. The viscosity data would indicate that there is no evidence that the hydroxyl reaction is having a significant effect on the overall reaction. If the hydroxyl reaction were to contribute significantly, the time to gelation at higher temperatures would be reduced, and there would be marked curvature in the viscosity curves prior to gelation.

4.2 SHARED MODEL SYSTEM

This system was a bisphenol-A-based (DGEBA) epoxy with 1,6-hexanediamine (HDA) as the curing agent. This aliphatic diamine curing agent differs from TETA in that it only has amine groups at the two chain ends, and therefore only has four

reactive hydrogen sites (two primary and two secondary). The consequent differences in the expected behaviour will be associated with a lower tendency to the creation of branched chain structures, but the greater flexibility imparted by the longer aliphatic segments between reactive species will be expected to increase reactivity. Prepared samples were cured at 45°C, 50°C, 55°C, 60°C, 65°C, 70°C and 75°C in the curemeter. For this particular system, lids were used on the vials as the amine was found to be volatile- as indicated by a clouding of the inside of the vial. The plastic lids were perforated to allow the paddle to move freely without interference.

The plots of the real and imaginary amplitudes from the curemeter measurements are given in Figure 5. The data set was converted to viscosity plots (Figure 6) and the times to gelation and vitrification for each temperature were calculated. As previously shown, the time taken to reach both gelation and vitrification decreased with increasing cure temperature. The amplitude plots are similar to those of the Strathclyde model system, with the exception that the real amplitude line does not fall through the imaginary peak maximum, but rather sits slightly to the right. The viscosity plots have a more hook-like shape at higher viscosities when compared to the relatively linear plots of the Strathclyde model system. However, they are still comparable below the defined gelation point (10^4 Pa s).

An interesting feature of the data is that the curves show a 'relaxation' effect at higher viscosities, where the plots increase to a maximum and then apparently decrease. This apparent relaxation effect is a consequence of the asymmetric nature of the phase shift plots and indicates a level of viscoelasticity in the material which will not necessarily be observed in other systems. This system has a longer aliphatic chain between the amine groups and it is probably that we are reaching a diffusion limited situation at gelation. After gelation the local exotherms will allow chain rearrangement and hence a softening of the matrix and also further reaction. The more highly functional TETA does not show this type of behavior.

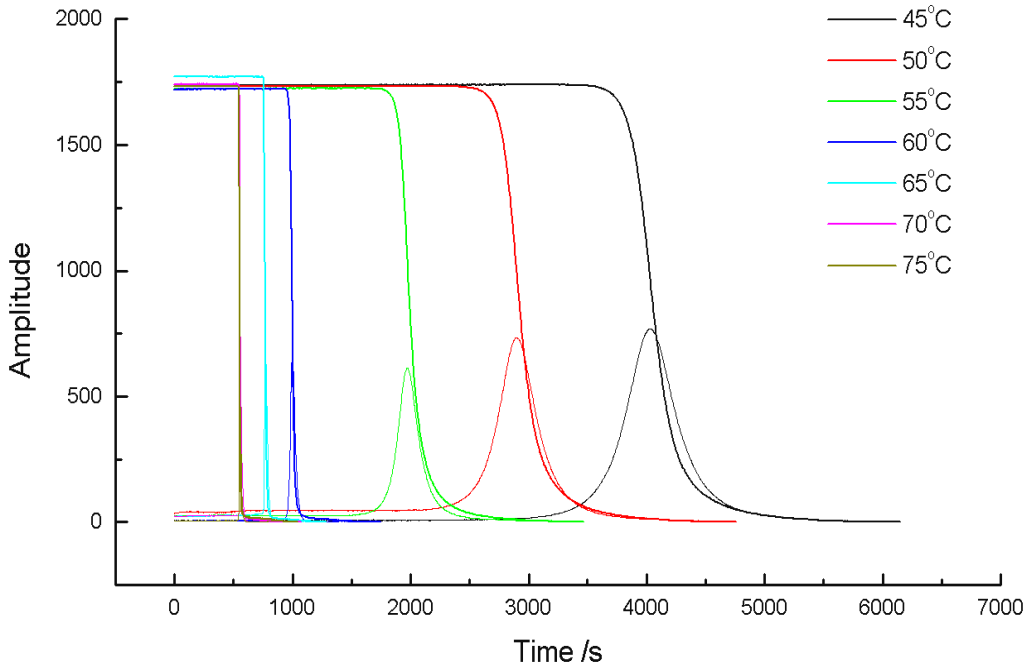

Figure 5. Amplitude plot against cure time, from curemeter data, for the shared model system at a range of cure temperatures.

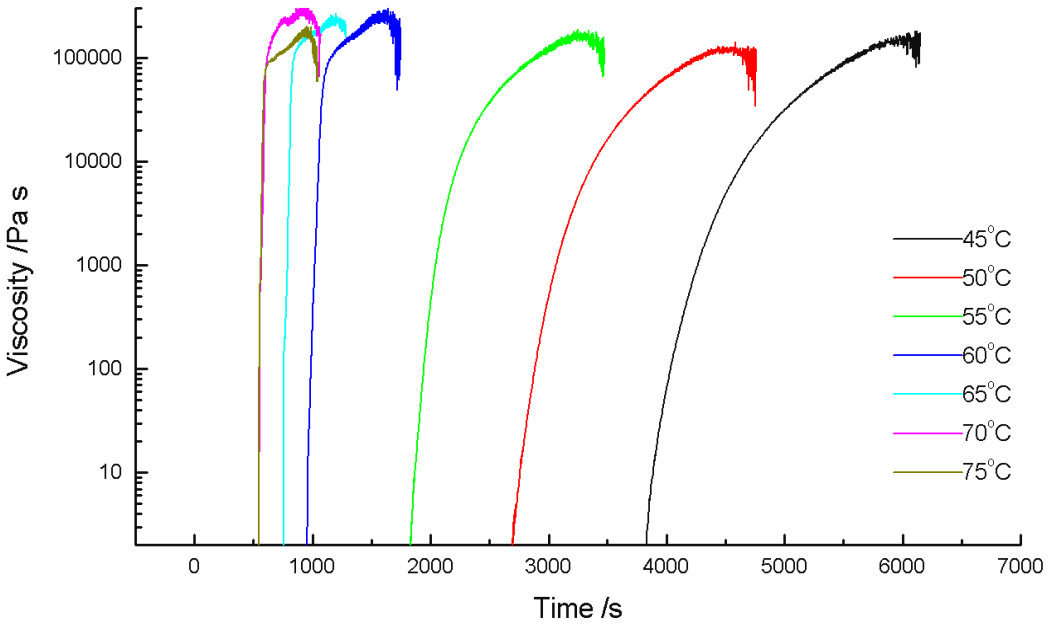

Figure 6. Viscosity profile plot against cure time, from curemeter data, for the shared model system at a range of cure temperatures.

The longer element of aliphatic chain between reactive groups will for the same degree of reaction as TETA produce a higher molar mass species. The observation of viscoelastic characteristics is consistent with the idea that polymer species are

undergoing chain entanglement before gelation. The absence of secondary amine in the curing agent will reduce the extent to which branched chain structures will be initially generated. Studies of the rheology of branched chain structures relative to linear structures of the same molar mass indicate that the branched chains tend to exhibit lower viscosities relative to the equivalent linear polymer which has a tendency to become involved in entanglement.

The times to gelation and vitrification are plotted in Figure 7 against the cure temperature. This plot shows decreasing cure time with increasing cure temperature, as can also be seen graphically in Figure 5. It can also be seen that the difference in the time to gelation (at 10^4 Pa s or at the peak maximum) and vitrification generally decreases with increasing cure temperature, with the exception of the difference for gelation and vitrification at 45°C which is lower than that of 50°C but higher than 55°C.

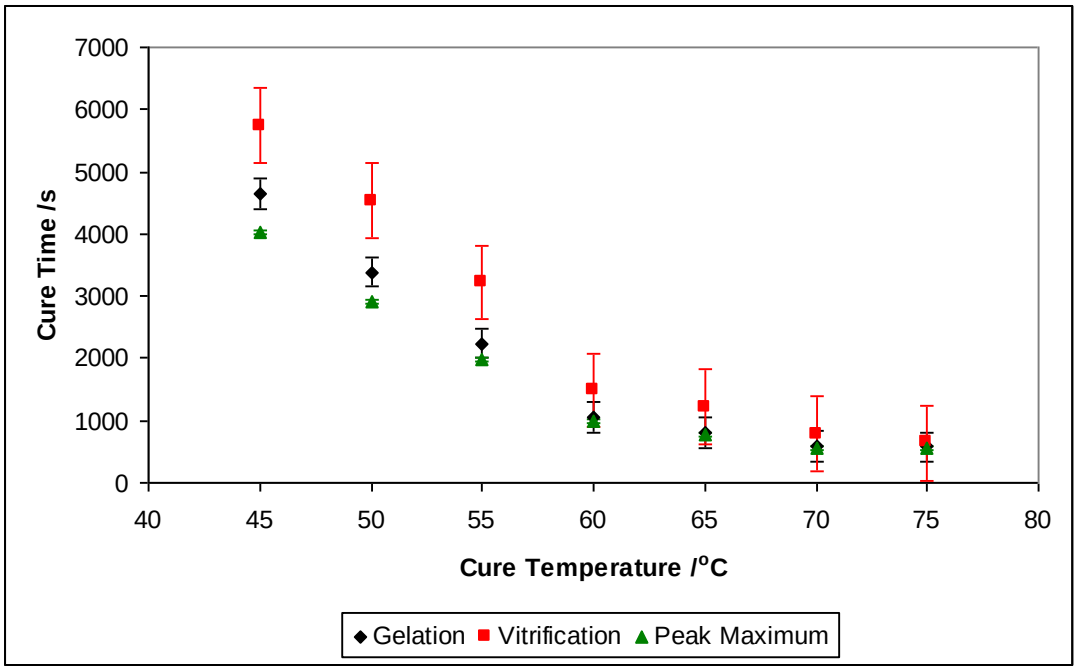

Figure 7. Plot showing affect of cure temperature on cure time for shared model system.

The observation of this apparent contradictory behaviour is consistent with the balance of temperature increasing the rate of reaction while the higher temperatures assist the chains in achieving a greater mobility and hence mobility is retained further

into the degree of conversion of the monomer. The activation energies (E_a) were calculated as previously detailed using the Arrhenius plot shown in Figure 8, and have values of:

$$\mathbf{E_a\ (gelation) = 71.2 \pm 2.0\ kJ\ mol^{-1}}$$

$$\mathbf{E_a\ (vitrification) = 72.7 \pm 5.0\ kJ\ mol^{-1}}$$

The activation energy for gelation when the cure time at the peak maximum is used is 67.2 ± 0.5 kJ mol^{-1}. The activation energy for this system is higher than that of the Strathclyde model system and probably reflects the lower level of the less reactive secondary amine present in the reaction mixture. In this system the ratio of primary to secondary amine is 1:1.

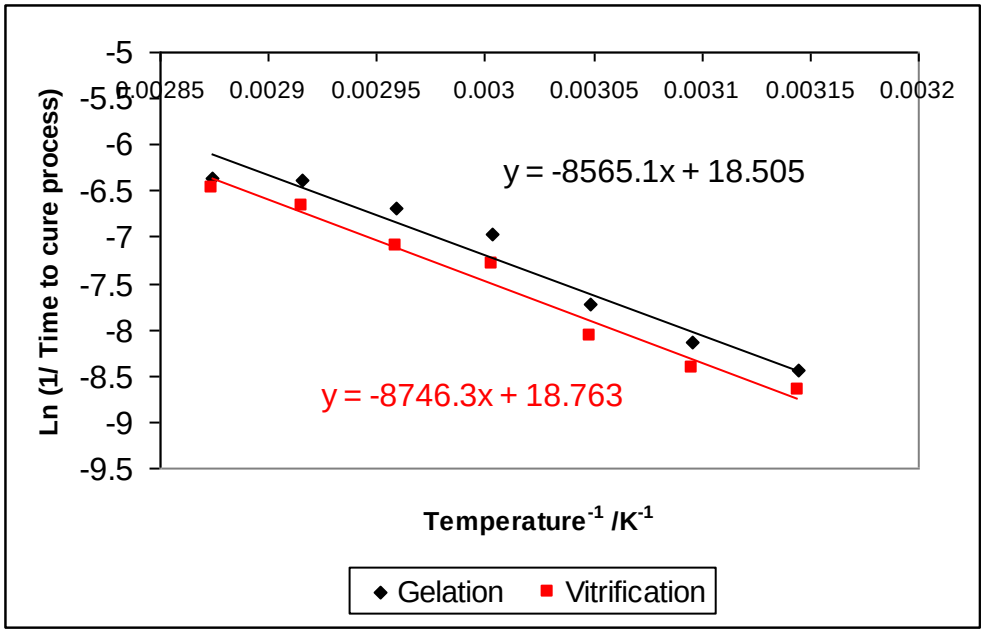

Figure 8. Arrhenius plot for the shared model system based on gelation and vitrification times calculated from shared model system curemeter data.

The rheology results show that small differences between the curing agent can influence the detail of rheological changes. However, the overall variation of the gelation time with temperature follows a simple Arrhenius type of behaviour.

4.3 SK31

Sikadur® 31, which is used to strengthen bridges and resembles wet cement in its uncured state, has a predominantly bisphenol-A-based (DGEBA) epoxy part cured with trimethylhexane-1,6-diamine- an aliphatic amine that is similar in structure to the 1,6- hexanediamine used in the shared model system. The epoxy component also contains some butanediol-diglycidyl ether which has an epoxy ring at the either end of the flexible chain and so can react in a similar way to DGEBA, except that it has a much shorter chain as it does not contain repeating units. Nonyl phenol is also present in the epoxy component, and is known to act as an accelerant [4] as it is a weak acid that can donate a proton to the amine.

The plots of the real and imaginary amplitudes, measured at 25°C, 30°C, 35°C, 40°C and 45°C, are given in Figure 9 below. The data set was converted to viscosity (Figure 10) and the time to gelation for each temperature was calculated. The amplitude plots are more similar to those of the Strathclyde model system as opposed to the shared model system as the real amplitude passes through the imaginary peak maximum. The viscosity plots show a different shape from that seen for the two model systems. It is thought that this is as a result of the filler(s) or accelerant(s) in the commercial system, however, the exact composition of the material was not provided with the material.

The curve at 30°C is exhibiting viscoelastic characteristics, whereas at higher temperatures the system appears to move more smoothly to gelation without an apparent indication of viscoelastic character. It is however evident that at all of the temperatures studied there is an almost immediate increase in the viscosity and this is consistent with the presence in the system of thickeners that are there to aid the processing of the resin. It is common practice in epoxy resins to use fumed silica as a thickening agent. The thickener will provide continuity through the fluid and this will give the resin an initial viscoelastic character.

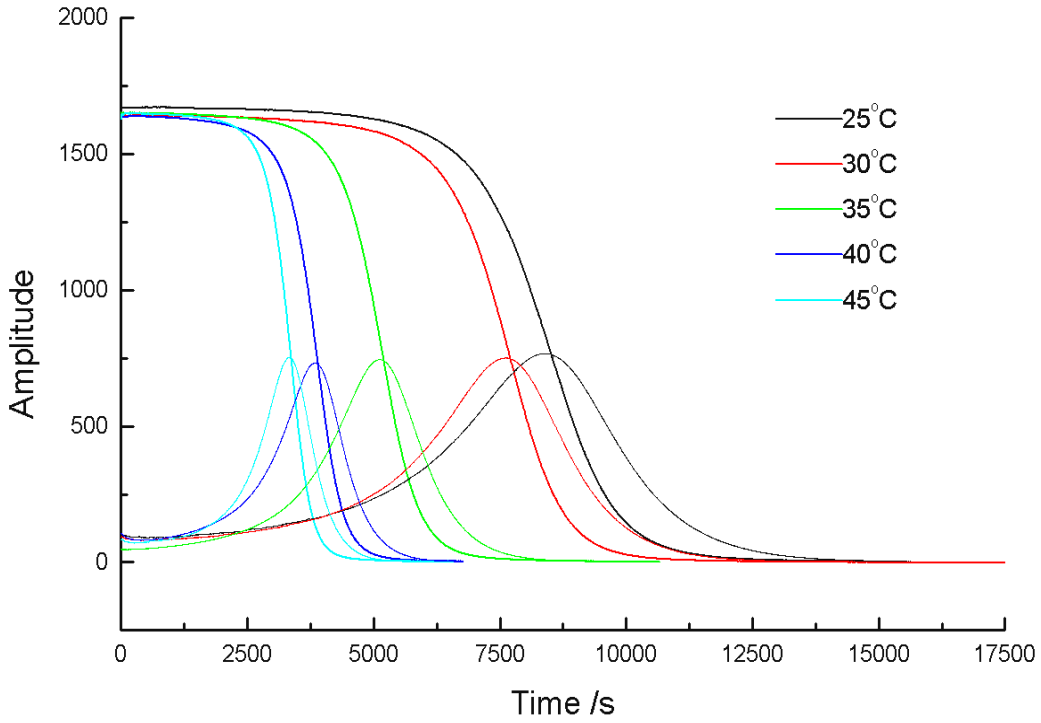

Figure 9. Amplitude plot against cure time, from curemeter data, for SK31 at a range of cure temperatures.

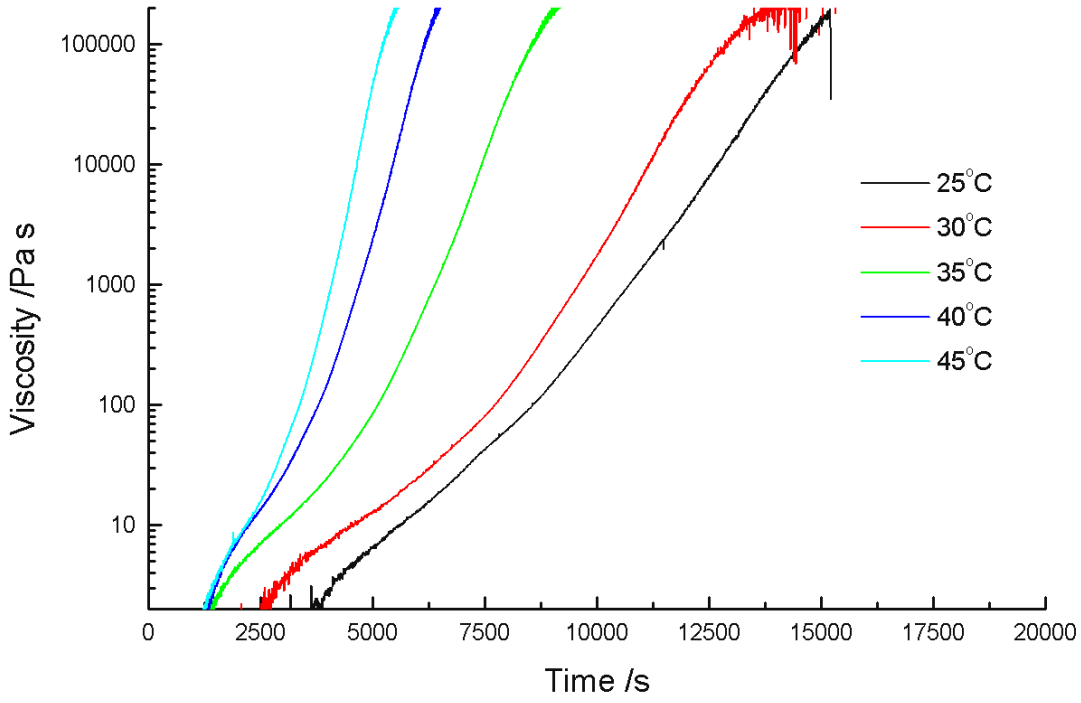

Figure 10. Viscosity profile plot against cure time, from curemeter data, for SK31 at a range of cure temperatures.

The shape of the viscosity–time plots show that there is a significant difference between these profiles and those demonstrated by the other mixtures. The principle difference between these systems is the presence, in this system, of the aliphatic linked epoxy material, different hardener, the presence of filler and the presence of hindered amines. The viscosity curves imply that there is initially a relatively fast reaction which is reduced to a slower rate for the final part of the cure. The apparent change in rate would imply that the aliphatic-based epoxy (butanediol-diglycidyl ether) may be consumed initially and that the aromatic-based material is left to the later stages of the reaction to be incorporated into the matrix. Alternatively, the surface activity of the filler could be influencing the reactivity, although this would most likely result in the resin having a pot life (whereby it would cure by itself). It is more probable that the interaction of the filler with the resin mixture is through interaction of the amine with silica surface, which will contain very few active hydroxyl groups.

The times to gelation and vitrification are plotted in Figure 11 against the cure temperature. This plot shows decreasing cure time with increasing cure temperature, as can also be seen graphically in Figure 9. It can also be seen that the difference in the time to gelation (at 10^4 Pa s or at the peak maximum) and vitrification generally decreases with increasing cure temperature. The variation of the cure time with temperature is not as smooth as with the previous two, simpler, systems. This may imply that there are different mechanisms contributing to the overall reaction.

The activation energies (E_a) were calculated as detailed previously- see Figure 12 for the Arrhenius plot. The activation energies were calculated to be:

$$\mathbf{E_a\ (gelation) = 43.0 \pm 2.0\ kJ\ mol^{-1}}$$

$$\mathbf{E_a\ (vitrification) = 41.6 \pm 5.0\ kJ\ mol^{-1}}$$

The activation energy for gelation when the cure time at the peak maximum is used is 39.9 ± 0.5 kJ mol^{-1}. It is clear that whilst there is now a complex reaction mechanism the overall characteristics of the cure are still following a relatively simple behaviour and fit the simple rate laws to a good approximation.

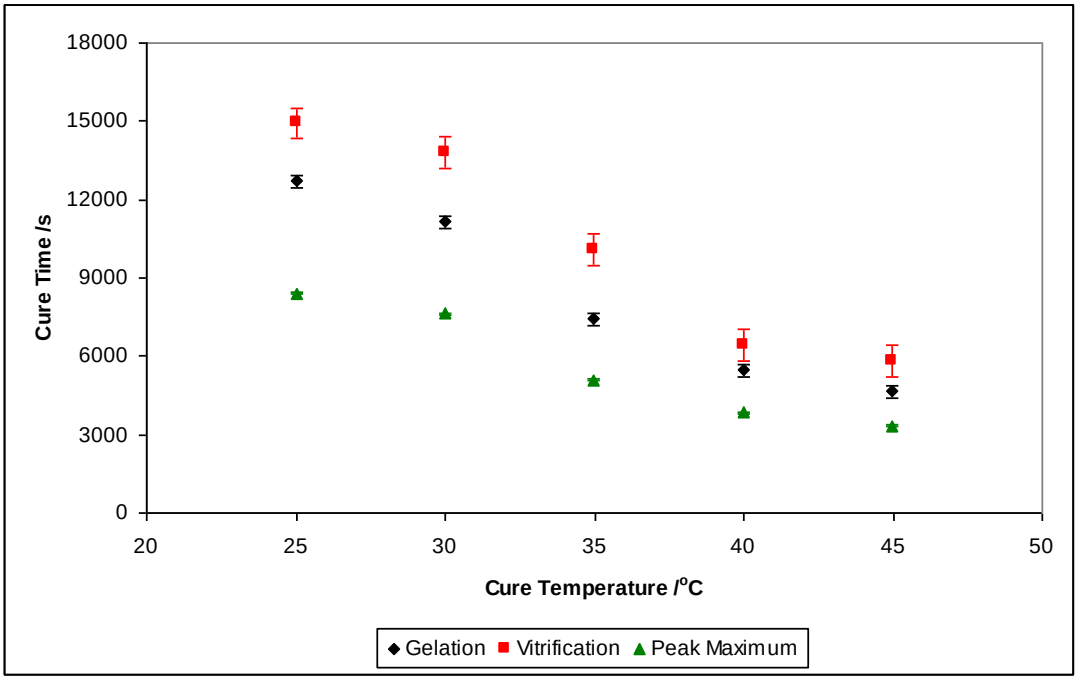

Figure 11. Plot showing affect of cure temperature on cure time for SK31.

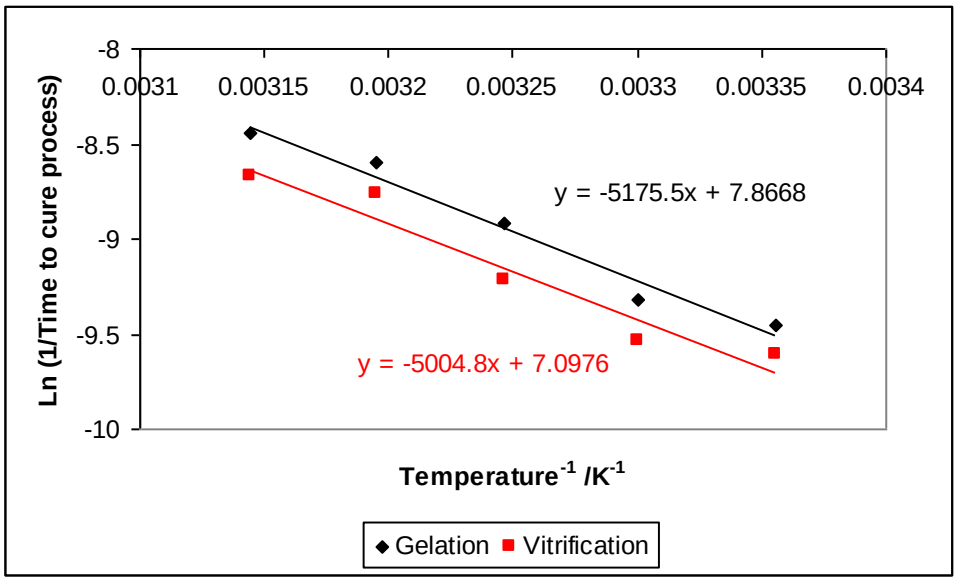

Figure 12. Arrhenius plot for SK31 based on gelation and vitrification times calculated from SK31 curemeter data.

4.4 PR55

PR55 is used industrially as the polymer matrix in carbon fibre composite patch repairs. The epoxy component is primarily bisphenol A (DGEBA)-based with some

diglycidylether of polypropyleneglycol, which has an epoxy end group at either end of the chain, and so can react in a similar way to DGEBA. However, the backbone chain does have repeating units, and so will be more like DGEBA than the butanediol-diglycidyl ether that is found in SK31. The hardener for this system is isophoronediamine with a smaller percentage of benzyl alcohol added. Isophoronediamine is an alicyclic amine with two primary and two secondary reactive hydrogens. Alcohols are often used with isophoronediamine as a plasticising diluent to reduce brittleness in the end product and can provide a weak accelerating effect during cure [5]. Benzyl alcohol is also known to act as a catalyst for the amine cure reaction when used with alicyclic amines.

The plots of the real and imaginary amplitudes, measured at 25°C, 30°C, 35°C, 40°C and 45°C, are given in Figure 13 below. The data set was converted to viscosity (Figure 14) and the times to gelation and vitrification for each temperature were calculated. The amplitude and viscosity plots are similar to the Strathclyde model system when curve shapes are compared. The times to gelation and vitrification are plotted in Figure 15 against the cure temperature. This plot shows decreasing cure time with increasing cure temperature and also that the difference in the time to gelation (at 10^4 Pa s or at the peak maximum) and vitrification generally decreases with increasing cure temperature. This resin system has a much lower initial viscosity than the SK31 system and is not filled. The viscosity-time plot shows some curvature prior to gelation which may be implied as the matrix beginning to build viscoelastic characteristics.

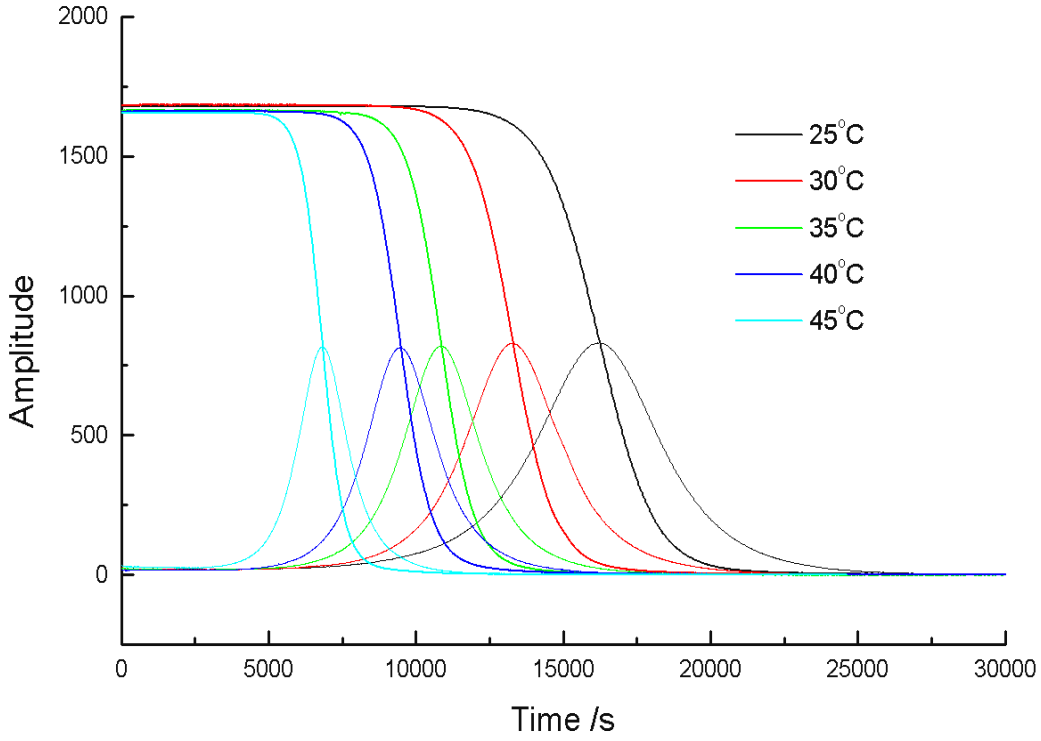

Figure 13. Amplitude plot against cure time, from curemeter data, for PR55 at a range of cure temperatures.

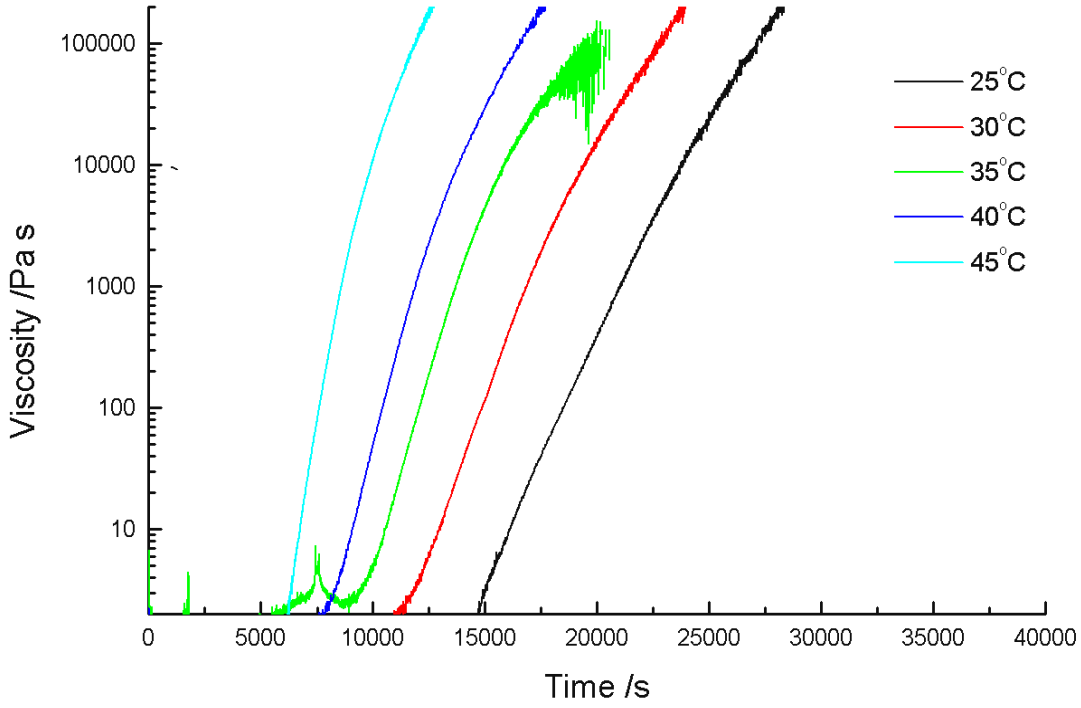

Figure 14. Viscosity profile plot against cure time, from curemeter data, for PR55 at a range of cure temperatures.

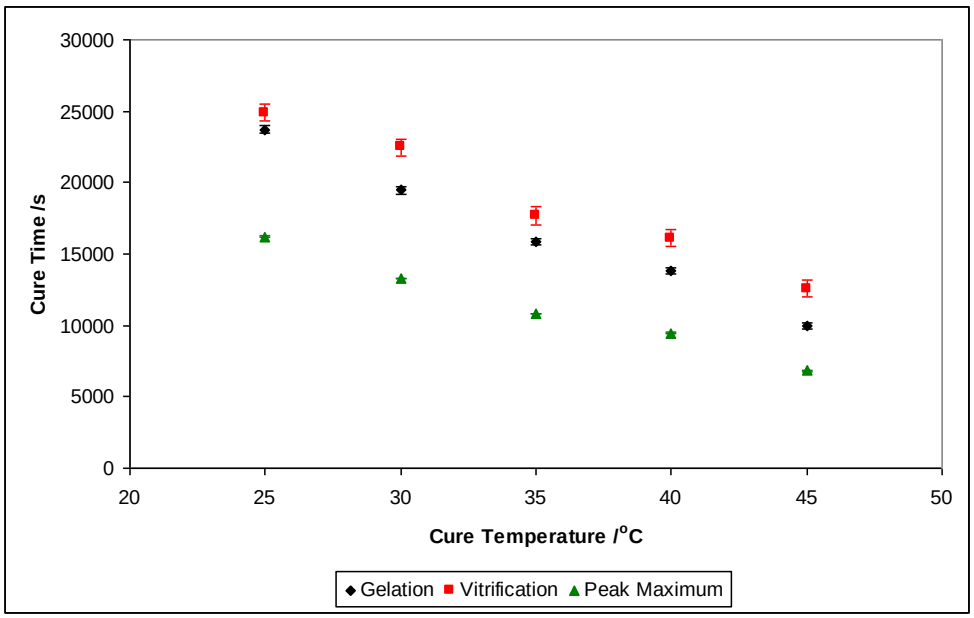

Figure 15. Plot showing effect of cure temperature on cure time for PR55.

The activation energy (E_a) was calculated as detailed previously- see Figure 16 for the Arrhenius plot. The activation energy calculated was found to be:

$$\mathbf{E_a\ (gelation) = 32.8 \pm 2.0\ kJ\ mol^{-1}}$$

$$\mathbf{E_a\ (vitrification) = 26.8 \pm 5.0\ kJ\ mol^{-1}}$$

The activation energy for gelation when the cure time at the peak maximum is used is 32.5 ± 0.5 kJ mol^{-1}.

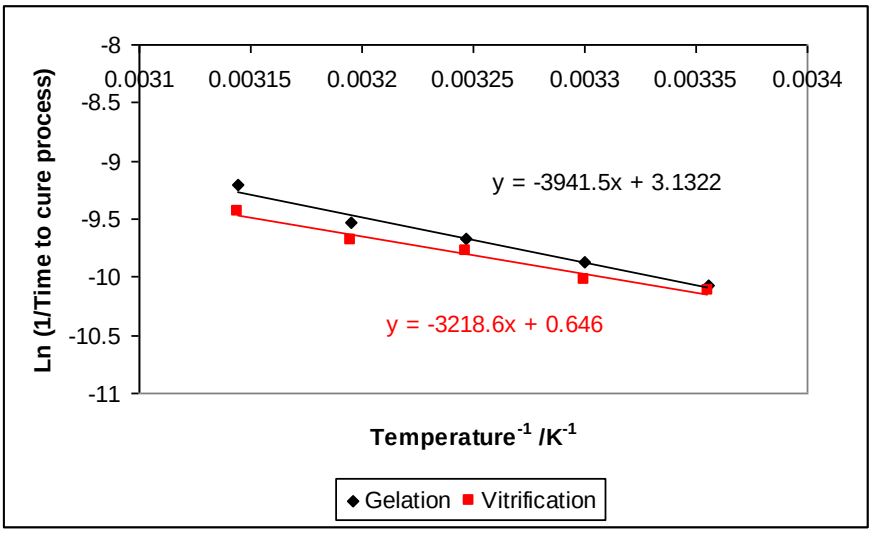

Figure 16. Arrhenius plot for PR55 based on gelation and vitrification times calculated from PR55 curemeter data.

The results imply that this system is demonstrating a higher reactivity than TETA and probably reflects the higher reactivity of the strained amine. The reactivity of this system appears to be fairly constant through the whole of the cure process.

4.5 PRIME20

Prime20 is used in a variety of resin infusion processes, including in the production of wind turbine blades. The epoxy component is predominantly bisphenol-A-based (DGEBA) with up to 25% DGEBF and a small amount of butanediol-digylcidyl ether. As previously described, although the diglycidyl ether has two terminal epoxy groups, it is a much shorter backbone chain when compared to DGEBA. C12/C14 alkylglycidyl ether is also present in quantities of less than 10%, and as this only has one epoxy group it is a reactive diluent that acts as a chain stopper- reducing functionality and hence reducing the cross-linking [4]. This constituent goes to the surface, while linked through the epoxy grouping to the polymer, and gives a smooth surface.

The hardener has various known constituents with the bulk being isophoronediamine (two each of primary and secondary hydrogens) and 2-piperazin-1-ylethylamine (one primary, one secondary plus one further secondary hydrogen attached to one of the nitrogens within the ring structure). There is also up to 25% polyoxyalkyleneamine (known as Jeffamine D) with terminal amine groups on a long linear chain, providing two primary and two secondary reactive hydrogens. The plasticising diluent, 4-*tert*-butylphenol, has been added due to the use of isophoronediamine in the system. In quantities of less than 2.5% the following two amines are also present and each contribute two primary and two secondary amines: *m*-phenylenebis methylamine and trimethylhexane-1,6-diamine - an aliphatic amine (similar to the hardener used in the shared model system).

The plots of the real and imaginary amplitudes, measured at 40°C, 50°C, 60°C, 70°C and 80°C, are given in Figure 17 below. The data set was converted to viscosity (Figure 18) and the times to gelation and vitrification for each temperature were

calculated. The amplitude and viscosity plots are similar to those of the Strathclyde model system, with the viscosity plots for PR55 being slightly more curved in the region after the defined gelation point (10^4 Pa s).

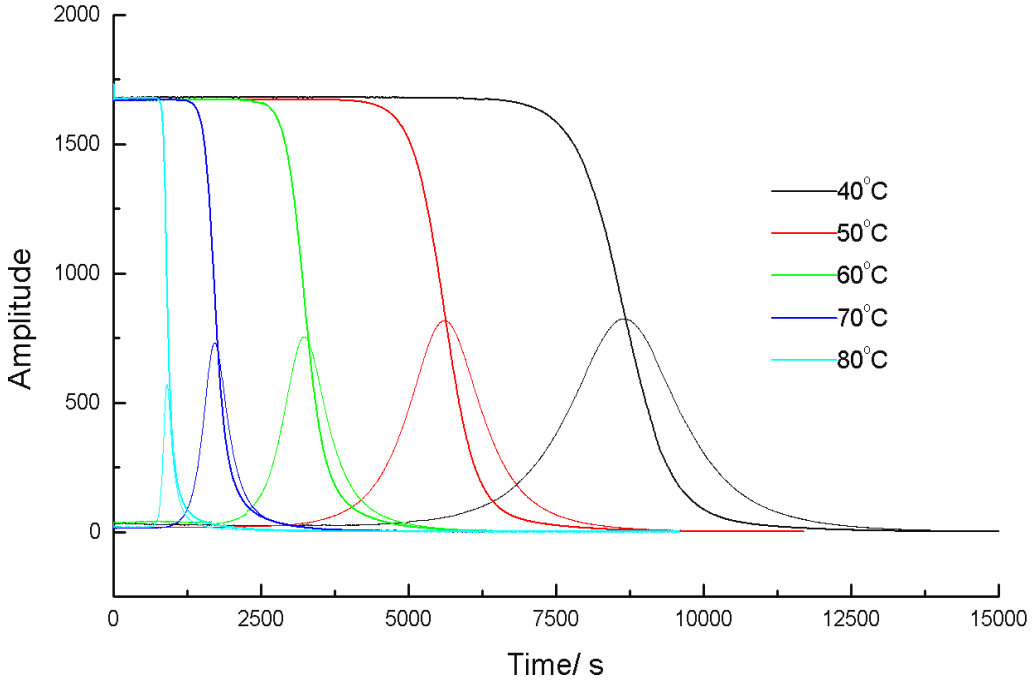

Figure 17. Amplitude plot against cure time, from curemeter data, for Prime20 at a range of cure temperatures.

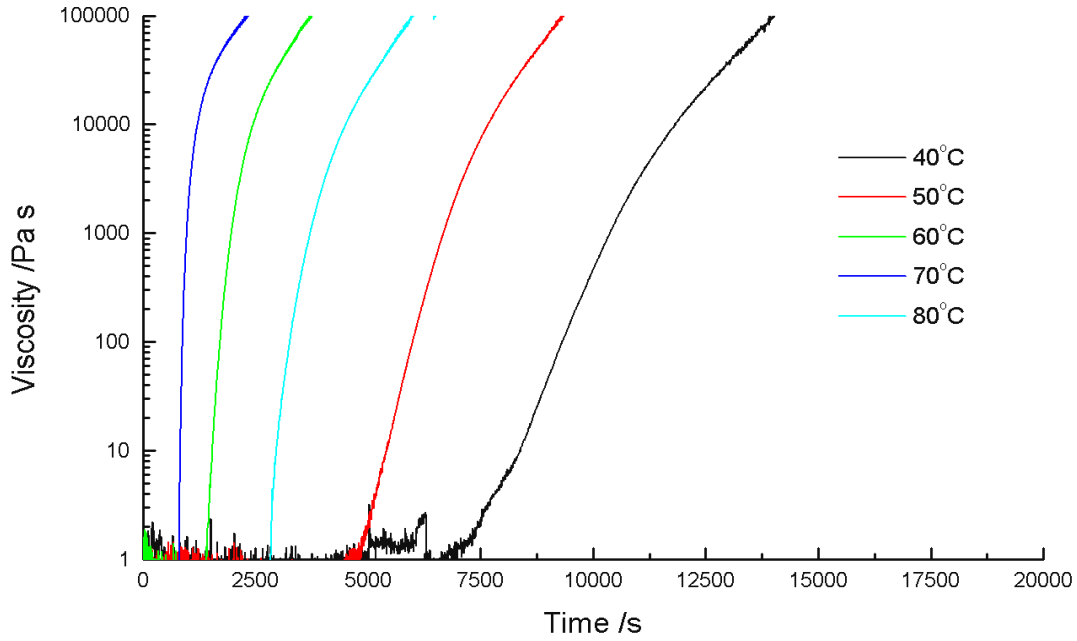

Figure 18. Viscosity profile plot against cure time, from curemeter data, for Prime20 at a range of cure temperatures.

The times to gelation and vitrification are plotted in Figure 19 against the cure temperature. This plot shows decreasing cure time with increasing cure temperature and also that the difference in the time to gelation (at 10^4 Pa s or at the peak maximum) and vitrification generally decreases with increasing cure temperature, with the exception that at the difference between gelation and vitrification at 40°C is smaller than that at 50°C, but larger than for 60°C.

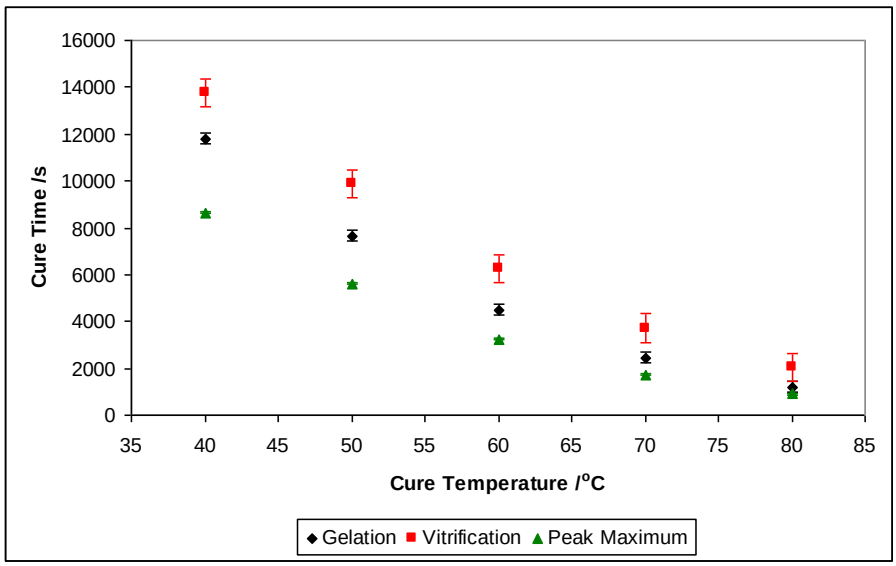

Figure 19. Plot showing effect of cure temperature on cure time for Prime20.

The activation energies (E_a) were calculated as detailed previously - see Figure 20 for the Arrhenius plot. The activation energies calculated from the curemeter measurements were found to be:

$$\mathbf{E_a\ (gelation) = 52.3 \pm 2.0\ kJ\ mol^{-1}}$$

$$\mathbf{E_a\ (vitrification) = 43.7 \pm 5.0\ kJ\ mol^{-1}}$$

The activation energy for gelation when the cure time at the peak maximum is used is 52.2 ± 0.5 kJ mol^{-1}.

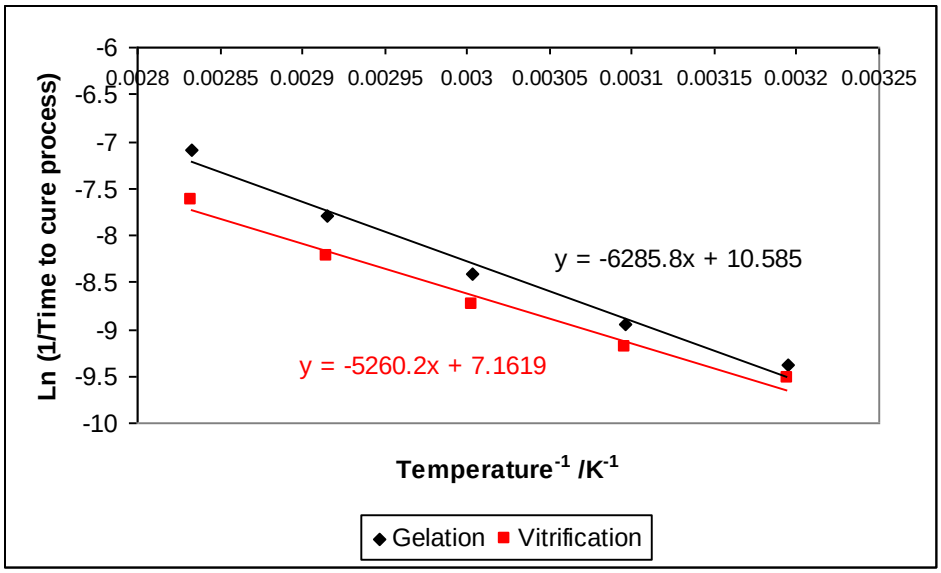

Figure 20. Arrhenius plot for Prime20 based on gelation and vitrification times calculated from Prime20 curemeter data.

The use of the mixed amine system is likely to be leading to the different type of kinetic operating over the cure period. The curves are showing a significant slow down in the build up of the viscosity as gelation is approached and evidence of a contribution of the relaxation of the matrix – diffusion control influencing the gelation process. However, the overall cure characteristics are similar to those of the other systems and obey simple temperature dependent characteristics.

4.6 SP340

Spabond SP340 is used as an adhesive in the manufacture of wind turbine blades. The epoxy component is primarily composed of DGEBA, with some butanediol diglycidyl ether (two terminal epoxy groups with a relatively short chain between), C12/C14 alkylglycidylether (only one terminal epoxy group with a chain about twice as long as that in the butanediol-diglycidyl ether), and epoxy novolac resin (three epoxy groups for reaction). The novolac resin increases the viscosity of the uncured resin. The alkylgylcidylether, with only one epoxy group, is a reactive diluent that is considered as a chain stopper as it reduces the functionality of the system, and hence the cross-linking is decreased [4]. This constituent goes to the surface, while linked through the epoxy grouping to the polymer, and gives a smooth surface.

The hardener is composed of up to 50% polyoxyalkyleneamine (Jeffamine D) which provides two each of primary and secondary reactive hydrogens. 2-piperazin-1-ylethylamine (previously described, with one primary and two secondary hydrogens) and isophorone diamine (two primary and two secondary hydrogens) are both present in quantities up to 10%, and benzyl alcohol and phenol are added as diluents which are plasticising in the presence of isophorone diamine. The TETA-like 3,6,9-triazaundecamethylenediamine is present at less than 0.5% and contributes two primary and five secondary hydrogens.

As has been previously noted, this system is difficult to work with as it is very viscous and does not de-gas well (in part due to the novolac). It was particularly difficult introducing the sample into the sample vial and it was felt that due to the tackiness of the material, when the paddle was inserted into the sample and allowed to oscillate, the material was dragged by the paddle and a true dampening may not be seen.

The plots of the real and imaginary amplitudes, measured at 25°C, 30°C, 35°C, 40°C, 50°C, 60°C, 70°C and 80°C, are given in Figure 21 below. The data set was converted to viscosity (Figure 22), and the times to gelation and vitrification for each temperature were calculated. As can be seen from the amplitude plot (Figure 21) all of the samples started at different values due to the difficult nature of the material.

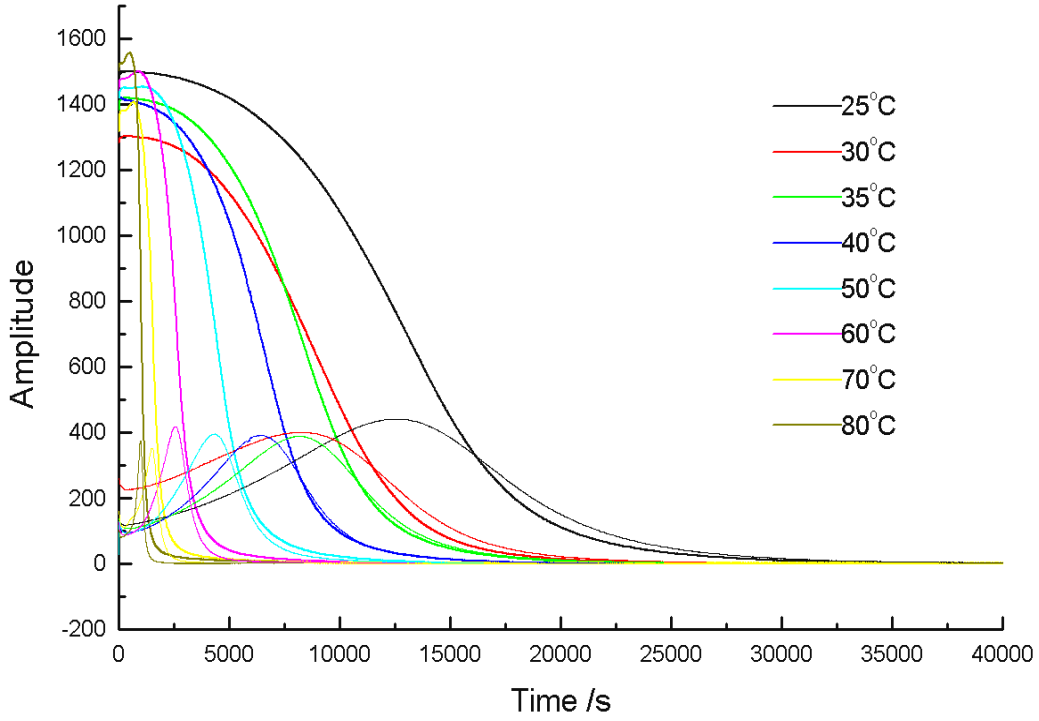

Figure 21. Amplitude plot against cure time, from curemeter data, for SP340 at a range of cure temperatures.

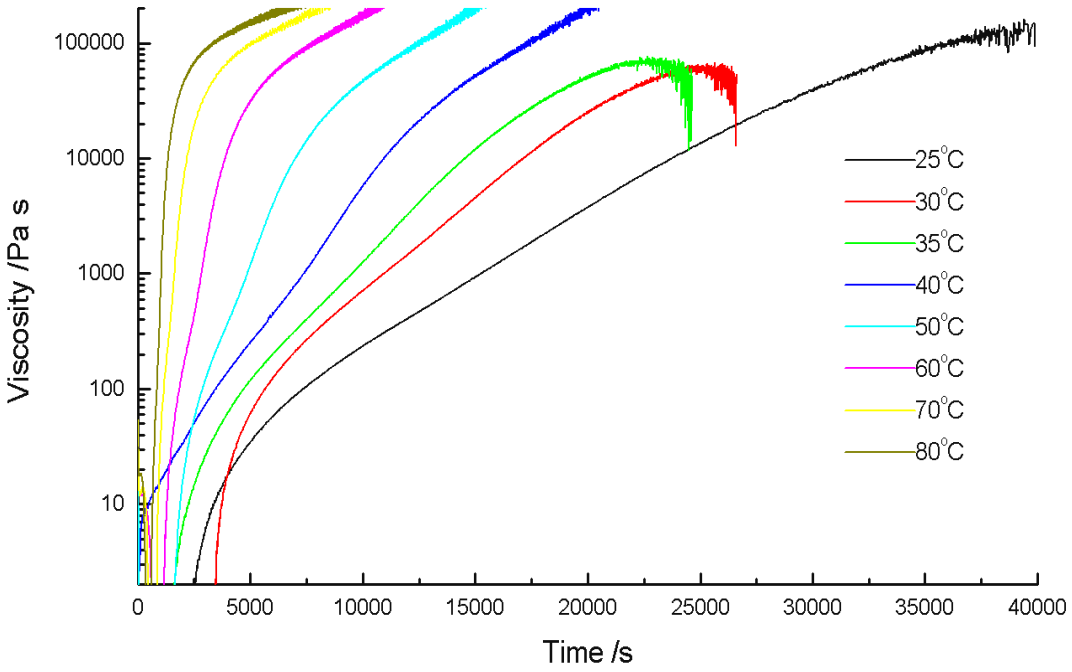

Figure 22. Viscosity profile plot against cure time, from curemeter data, for SP340 at a range of cure temperatures.

The viscosity plots (Figure 22), show quite a different curve shape compared to the other systems, and several of the lines overlap. However, when the viscosity has reached approximately 10^2 Pa s the lines are spaced out as expected with increasing cure temperatures showing decreasing time to a particular viscosity, allowing the activation energy to be calculated. The times to gelation and vitrification are plotted in Figure 23 against the cure temperature. This plot shows decreasing cure time with increasing cure temperature and also that the difference in the time to gelation (at 10^4 Pa s or at the peak maximum) and vitrification generally decreases with increasing cure temperature.

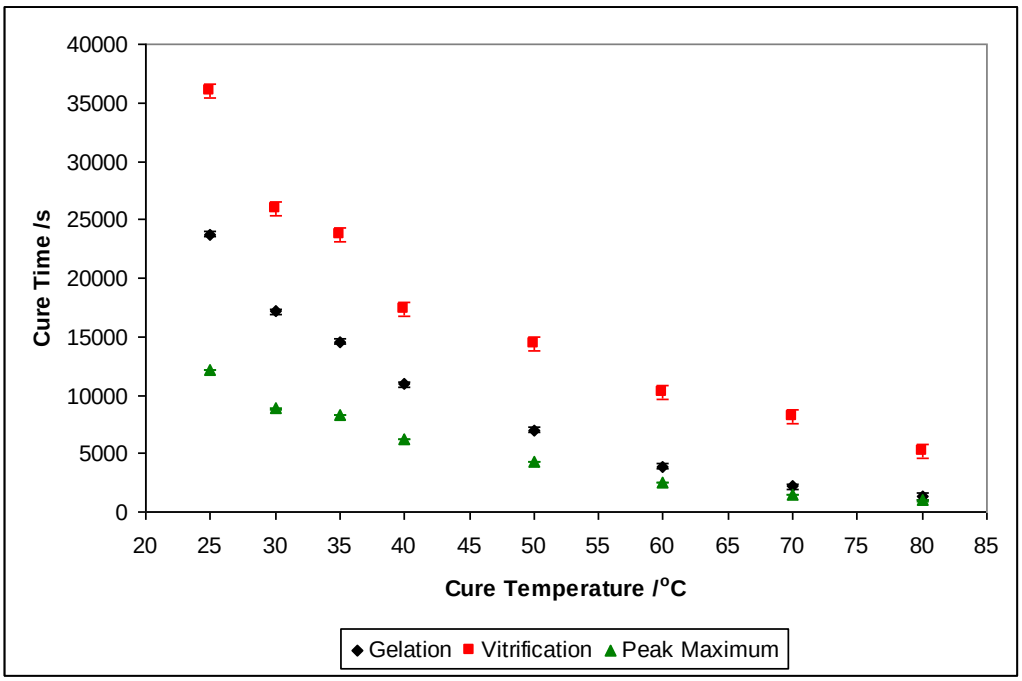

Figure 23. Plot showing effect of cure temperature on cure time for SP340.

The activation energies (E_a) were calculated as detailed previously - see Figure 24 for the Arrhenius plot - and found to be:

$$\mathbf{E_a\ (gelation) = 45.5 \pm 2.0\ kJ\ mol^{-1}}$$

$$\mathbf{E_a\ (vitrification) = 28.3 \pm 5.0\ kJ\ mol^{-1}}$$

The activation energy for gelation when the cure time at the peak maximum is used is 39.9 ± 0.5 kJ mol^{-1}.

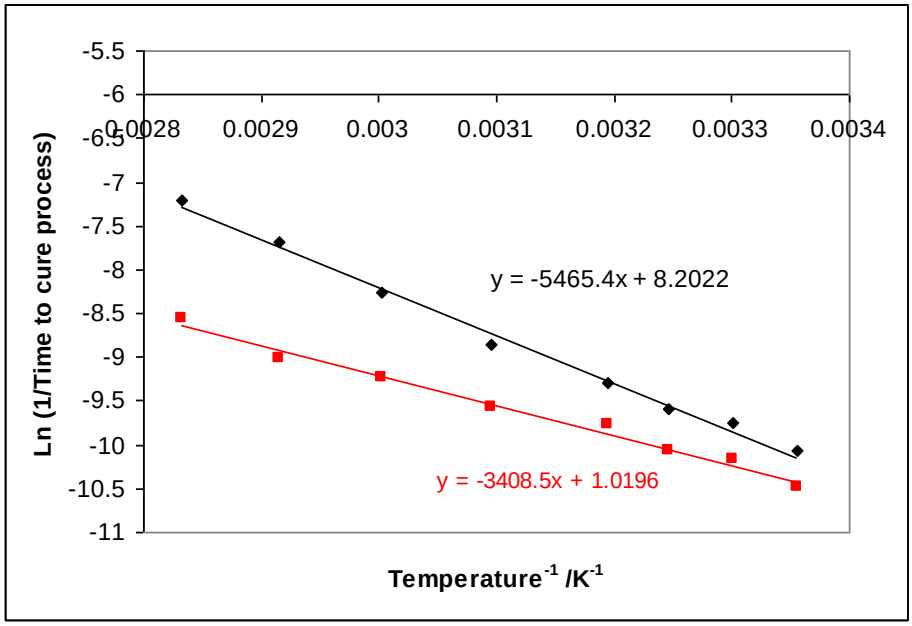

Figure 24. Arrhenius plot for SP340 based on gelation and vitrification times calculated from SP340 curemeter data.

This complex mixture shows through the viscosity curves changes in the rate at which the cure process occurs. The observed curves deviate from the simple linear variation found in TETA and show a series of discernable changes before gelation occurs reflecting the different reactivities of the components present. Despite the complexity of the cure process the overall rate of cure shows a simple dependence in terms of good linear activation plots and a simple variation with temperature.

4.7 CONCLUSIONS

All of the systems were studied using the Strathclyde curemeter to monitor viscosity changes with cure time. Gelation was defined as occurring at 10^4 Pa s, and the time it took to reach this value was termed the gel time. The systems all showed decreasing gel time with increasing cure temperature as expected. The SP340 system was particularly difficult to work with and it is thought that the true dampening effect was not reflected in these results, although by approximately 10^2 Pa s the material did at least show the trend relating cure temperature and gel time.

The activation energies calculated are shown in Table 1 below.

Table 1. Activation Energy values (gelation, vitrification and average) for each system calculated from Strathclyde curemeter measurements.

System	E_a (gel) /kJ mol^{-1} (± 2.0 kJ mol^{-1})	E_a (vit) /kJ mol^{-1} (± 5.0 kJ mol^{-1})
Strathclyde Model	50.5	47.5
Shared Model	71.2	72.7
Sikadur® 31	43.0	41.6
PR55	32.8	26.8
Prime20	52.3	43.7
Spabond SP340	45.5	28.3

Where Ea (gel) is for gelation; Ea (vit) is for vitrification.

There are significant variations in the calculated activation energies between the systems studied. The lowest activation energy and hence fastest to cure is the PR55 system. This mixture contains an aliphatic epoxy and the catalyst benzyl alcohol in addition to the usual aromatic epoxy resin, where the reactivity of the aliphatic epoxy is able to assist the cure of the aromatic-based epoxy resin. The Prime20 system also has a similar blend of the aliphatic and aromatic-based epoxy resins and also a blend of amines, but lacks the benzyl alcohol catalyst and as a consequence the activation energy is significantly higher. The Spabond SP340 system contains the catalyst but also contains a significant amount of the novolac-based epoxy which has raised the viscosity and is clearly having an effect on the activation energy. The value being lower than for the Prime20 system but significantly higher than the PR55. The SK31 system contains some of the aliphatic epoxy but has the nonyl phenol as a catalyst. The activation energy is higher than the case when benzyl alcohol is present as a catalyst (PR55) but slightly lower than for the Spabond SP340 for gelation. The Strathclyde model and shared model systems both show high activation energies, both systems are uncatalysed and the epoxy is a simple aromatic-based material. Comparison of the systems indicates the significant increase in reactivity which can be achieved by the incorporation of a small proportion of aliphatic-based epoxy resins in the system. These molecules will be able to diffuse through the matrix more easily than the aromatic-based epoxy resins and hence are able to achieve reaction

more efficiently than the aromatic-based materials. The study also illustrates the catalytic activity of the benzyl alcohol and phenol and their ability to significantly promote reaction.

Despite the significant differences in the chemistry involved in the cure the systems stay surprisingly well behaved and analysis for the cure data conforms to a simple Arrhenius description of the kinetics and implies that despite the molecular complexity of the system, the overall kinetics can be simply described in terms of gross reactivity constants. This observation suggests that it may be possible to use simple probes to map the cure process for many different epoxy resin systems.

4.8 REFERENCES

1. Hayward, D., R.A. Pethrick, B. Eling, and E. Colbourn, *Prediction of the Rheological Properties of Reactive Polymer Systems.* Poly Int, 1997. **44**: p. 248-254.

2. Affrossman, S., A. Collins, D. Hayward, E. Trottier, and R.A. Pethrick, *A versatile method of characterising cure in filled reactive polymer systems.* Journal of the Oil & Colour Chemists Association, 1989. **72**(11): p. 452-454.

3. Pethrick, R.A., *Chapter 3: Rheological Studies Using a Vibrating Probe*, in *Rheological Measurement*, A.A. Collyer and D.W. Clegg, Editors. 1998, Chapman & Hall: London.

4. Potter, W.G., *Epoxide Resins*. 1970, London: Butterworth & Co.

5. Ashcroft, W.R., *Chapter 2: Curing agents for epoxy resins*, in *Chemistry and Technology of Epoxy Resins*, B. Ellis, Editor. 1993, Blackie Academic & Professional: Glasgow.